J. Ind. Geophys. Union (September 2018)
v.22, no.5, pp: 485-506

Possible seismic hazards in Chandigarh city of North-western India due to its proximity to Himalayan frontal thrust

Nitish Puri[1]* and Ashwani Jain[1]
[1]Department of Civil Engineering, NIT Kurukshetra, Kurukshetra, Haryana – 136119, India
*Corresponding author: nitishpuri.ce.89@gmail.com

ABSTRACT
Chandigarh, the first ever planned city in India, currently having an urban agglomeration of 1.2 million, is situated in the proximity of the Himalayan Frontal Thrust (HFT) zone. It falls under the seismic zone IV as per IS 1893 Part-1 (2016). It is ranked as second most seismically vulnerable city in India, based on expected peak ground acceleration (PGA) as per National Disaster Management Authority (NDMA). In the present study, the results of seismic hazard analysis for Chandigarh city, carried out adopting probabilistic approach are reported. The PGA values are estimated for rock sites, and a seismic hazard map for the city is prepared. Based on the observed PGA values, one-dimensional nonlinear wave amplification analysis and liquefaction potential assessment are also made. For this purpose, geotechnical data are collected for 41 boreholes from various government and private organizations, to have an assessment of soil properties and ground water conditions. For the sites under consideration, it is observed that ground motions get amplified at 5 sites due to local site effects and 18 sites in the city are prone to liquefaction. Therefore, a site-specific design approach should be adopted in the city for the design of important structures at vulnerable sites.

Keywords: Probabilistic seismic hazard, wave amplification, liquefaction potential, Himalayan thrust system.

INTRODUCTION

Earthquake is an event which can inflict severe damage to the infrastructure of a city and take it back to a few decades. The recent example is the Canterbury earthquakes of 2010 and 2011 that caused heavy damages in the Christchurch city of New Zealand. The estimated cost to rebuild is around 20% of total GDP of New Zealand, i.e. about NZ$40 billion approximately (Potter et al., 2015). Similarly, in 2001 Bhuj earthquake, total property damage was estimated at about $7.5 billion. The multi-storey structures in Ahmedabad city, being located on younger alluvial deposits, experienced heavy damage, inspite of greater distance of the city (more than 300 km) from the earthquake epicenter (Ranjan, 2005). Hence, it is necessary for areas located in the vicinity of tectonically active sources to be ready with proper mitigation measures and rescue arrangements, for example cities close to Himalayan range, which were formed due to the collision between Indian plate and Asian plate that are still converging at a rate of 55 mm/year (Peltzer and Saucier, 1996). The earthquakes occurring in this region are due to the formation and uplift of the mountains.

The Himalayan thrust system, consisting (from north to south) the Main Central Thrust (MCT), the Main Boundary Thrust (MBT) and the Himalayan Frontal Thrust (HFT), are considered one of the most seismically active tectonic zones in the world (Malik et al., 2010). This has been demonstrated by the occurrence of several large magnitude earthquakes in the area (Table 1). It is believed that since the 1897 Shillong earthquake of M_w 8.0, the Himalayan region seems to have ruptured ranging from 15 to 20% to as much as 45%, and the risk of an imminent great earthquake is thus high (e.g. Molnar and Pandey, 1989). Moreover, the central Himalaya, which is considered as a prominent 'seismic gap' (Khattri et al., 1984), is believed to be the most vulnerable segment and is due for a great plate boundary earthquake of greater than M_w 8.0 (Rajendran and Rajendran, 2005). A large area adjacent to the Himalayan thrust system may be subjected to severe damage during an earthquake.

The geographical location of the Chandigarh city, which is located in the Himalayan foothills to the south of HFT, makes it susceptible to huge damage due to earthquakes in the Himalayan thrust system (MCT, MBT and HFT). Moreover, the alluvial land cover also makes it prone to hazards due to wave amplification and soil liquefaction. The gradual increase in population density has also increased vulnerability of the city. This calls for an immediate site-specific seismic hazard analysis (SHA) and estimation of other earthquake induced hazards. Besides, the damage inflicted by the large earthquakes in this region which occurred earlier (Table 1), also calls for taking appropriate mitigation measures.

In the present study, possible seismic hazards in the city of Chandigarh have been evaluated. It includes estimation of seismic hazard by probabilistic seismic hazard analysis, wave amplification analysis and determination of liquefaction potential. Results have been formulated in terms of seismic hazard maps for various return periods, response spectra, peak ground acceleration amplification factors and a liquefaction hazard map.

Table 1. Major earthquake events in the Himalayan thrust system (source: en.wikipedia.org).

Earthquake	Date	Magnitude	Damage report
1905 Kangra earthquake	4 April 1905	7.8 M_s	Death toll: 20,000 Massive destruction of structures
1934 Bihar–Nepal earthquake	15 January 1934	8.0 M_w	Death toll: 12,000 Massive damage to structures, roads and telephone lines
1950 Assam earthquake	15 August 1950	8.6 M_w	Death toll: 4,800 Massive landslides,70 villages destroyed
2005 Kashmir earthquake	8 October 2005	7.6 M_w	Death toll: 87,000 Massive damage to structures, 75,000 injured and 2.8 million displaced
2015 Gorkha earthquake	25 April 2015	7.8 M_w	Death toll: 9,000 Massive damage to structures, 24,000 injured and 3.5 million homeless

REVIEW OF LITERATURE

Seismic hazard analysis is the first step towards mitigation of earthquake hazards. It is carried out for quantitative evaluation of expected earthquake hazard at a site. Two approaches, probabilistic (PSHA) and deterministic (DSHA), are commonly adopted for seismic hazard assessment. In DSHA, a particular earthquake scenario is assumed, based on past data and tectonic set up of the study area, and hazard is estimated based on attenuation characteristics of the region. The DSHA provides the worst-case scenario earthquake that can occur in the region and the strong-motion parameters are estimated for the maximum credible earthquake assumed to occur at the closest possible distance from the site of interest. This is done without considering the likelihood of its occurrence for a specified exposure period during the design life of the structure. It is used widely for nuclear power plants, large dams, large bridges, hazardous waste containment facilities and as a 'cap' for PSHA (e.g. Puri and Jain, 2016). Several studies have been carried out in India based on this approach; for example, Chennai city (Boominathan et al., 2008), Gujrat region (Chopra et al., 2012), Kolkata city (Shiuly and Narayan, 2012), India (Kolathayar et al., 2012a), major cities of Gujrat (Shukla and Choudhury, 2012), Andaman and Nicobar Islands (Kataria et al., 2013), Goa (Naik and Choudhury, 2015) and Haryana (Puri and Jain, 2016).

On the contrary, PSHA rectifies several problems inherent in its deterministic analysis, viz. lack of quantification of uncertainties in size, location of an earthquake and probability of its occurrence. It quantitatively represents the relationship between potential seismic sources, associated ground motion parameters and respective probabilities of occurrence. It also computes the probability of exceeding of specified level of ground motion at a particular site, which is represented as function of return period and fault displacement. Due to its capability to accommodate uncertainties, more and more seismic hazard analyses are being carried out using probabilistic approach (e.g. for Delhi by Sharma et al., 2003; Tripura and Mizoram states by Sitharam and Sil, 2014; Surat city by Thaker et al., 2012; Patna by Anbazhagan et al., 2015a). However, the present DSHA and PSHA methodologies account for the earthquake hazard for rock sites only and the effect of wave amplification is rarely considered in ground motion models. Therefore, identification of soil layers susceptible to ground motion amplification is an important task for accurate assessment of seismic hazard in earthquake prone areas. The development of site specific ground motions involves the study of both seismic hazard and wave amplification.

It is known that the wave amplification, soil liquefaction, landslides and tsunami are the most devastating after-effects of an earthquake. However, landslides and tsunami can only be observed in hilly and coastal areas respectively, thereby making the first two, i.e. seismic wave amplification and soil liquefaction as the crucial parameters observed in plain areas, where the earthquake manifests itself as shaking of ground and sometimes its displacement. Earthquake engineers are primarily interested in the strong ground motions which are sufficiently strong to be felt during an earthquake.

Table 2. Magnitude conversion equations.

Source	Conversion Equations
Scordilis (2006)	$M_w = 0.67\ M_s + 2.07$, for $(3.0 \le M_S \le 6.1)$ $M_w = 0.99\ M_s + 0.08$, for $(6.2 \le M_S \le 8.2)$
Scordilis (2006)	$M_w = 0.85\ m_b + 1.03$, for $(3.5 \le m_b \le 6.2)$
Kolathayar, Sitharam and Vipin (2012b)	$M_w = 0.815\ M_L + 0.767$, for $(3.3 \le M_L \le 7.0)$
Yenier, Erdoğan and Akkar (2008)	$M_w = 0.764\ M_d + 1.379$, for $(3.7 \le M_d \le 6.0)$

M_s-surface wave magnitude, m_b-body wave magnitude, M_L-local magnitude, M_d-duration magnitude

Characteristics of seismic waves get modified as they travel through different soil conditions. This phenomenon is referred to as 'local site effects'. Local site conditions have profound influence on all the important seismic characteristics, i.e. amplitude, frequency content and duration of strong ground motions. The extent of influence depends upon thickness and properties of the soil cover, site topography, and on the characteristics of the input motion itself. The phenomenon of wave amplification due to local site effects has been well demonstrated, in case of many earthquakes , like 1985 Michoacán, Mexico earthquake M_w 8.0, the 1989 Loma Prieta, San Francisco earthquake M_w 6.9, the 2000 Totoriken-seibu, Japan earthquake M_w 6.7 (Kramer, 2013), the 1999 Chamoli earthquake M_w 6.8 (Nath et al., 2002) and the 2001 Bhuj earthquake M_w 7.6 (Ranjan, 2005).

Similarly, the phenomenon of loss of strength of loose saturated cohesionless soils subjected to dynamic loading due to increase in pore water pressure is termed as soil liquefaction. It is manifested in the form of sand boils and mud spouts at the ground surface formed by seepage of water, or in some cases by the development of quick sand condition. In such cases, buildings may sink substantially into the ground or tilt excessively; lightweight structures and foundations may get displaced laterally causing structural failures. Such phenomenon was well demonstrated for several earthquakes around the world, for example, the 1934 Bihar-Nepal earthquake M_w 8.2, the 1964 Niigata, Japan earthquake M_w 7.6, the 2001 Bhuj, western India earthquake M_w 7.6 and the 2011 Christchurch, New Zealand earthquake M_w 6.3. Hence, it is important to assess liquefaction potential of the susceptible soils that plays a major role for seismic hazards. An initial screening of whether the site would undergo liquefaction can be done on the basis of various factors such as geology of the area, depth of ground water table, grain size distribution etc. (Puri and Jain, 2014). For example, loose, fine, saturated and poorly graded sands are more susceptible to liquefaction in comparison to dense and well-graded soils. However, a detailed assessment of liquefaction susceptibility requires analysis of stresses induced by the earthquake and resistance offered by the soil deposit. Various semi-empirical methods have been reported based on SPT N-value, shear wave velocity (V_s), cone penetration resistance etc. (e.g. Tokimatsu and Uchida, 1990; Youd et al., 2001; Cetin et al., 2004; Idriss and Boulanger, 2006).

SEISMOTECTONICS OF THE STUDY AREA

Chandigarh city is located at the foothills of Himalayas, occupying an area of 120 km^2. It is a Union Territory and common capital of the states of Haryana and Punjab. The city falls under Seismic Zone IV as per IS 1893 Part-1 (2016). It is located along Himalayan Thrust System and is considered to be highly prone to earthquakes. Paleo-seismic investigations across the Chandigarh fault in the frontal Himalayan region reveal that two major earthquakes occurred during the 15^{th} - 16^{th} century (Malik et al., 2008).

Development of earthquake catalogue and tectonic map

An area covering 300 km around Chandigarh (30.73° N, 76.77° E) has been considered as the study area. A comprehensive earthquake catalogue for a period from January 1291 to September 2016 (~725years) has been compiled, using data collected from various national and international seismological agencies, like National Disaster Management Authority (NDMA), India Meteorological Department (IMD), International Seismological Center (ISC-UK) and United States Geological Survey (USGS). The catalogue comprises of 2160 earthquake events of magnitude $M_w \ge 4$ in the region (Lat 28^o-$33^o.5$ N and Long $73^o.5$-80^o E). The catalogue has been carefully homogenized to a common scale of moment magnitude (M_w) and de-clustered to remove dependent events like foreshocks and aftershocks. Homogenization has been carried out using equations as reported in Table 2.

Declustering is carried out considering space and time windows proposed by Gardner and Knopoff (1974) which are: Distance=$e^{-1.024+0.804M}$ and Time=$e^{-2.87+1.235M}$. Some 142 dependent events are removed and an epicenter map for the study area is prepared (Figure 1).

The catalogue is examined for completeness. For this purpose, catalogue is divided into several magnitude classes, and completeness periods are calculated using Cumulative Visual Inspection (CUVI) method of Tinti and Mulargia (1985), and Stepp (1972) method as shown in Figure 2 and

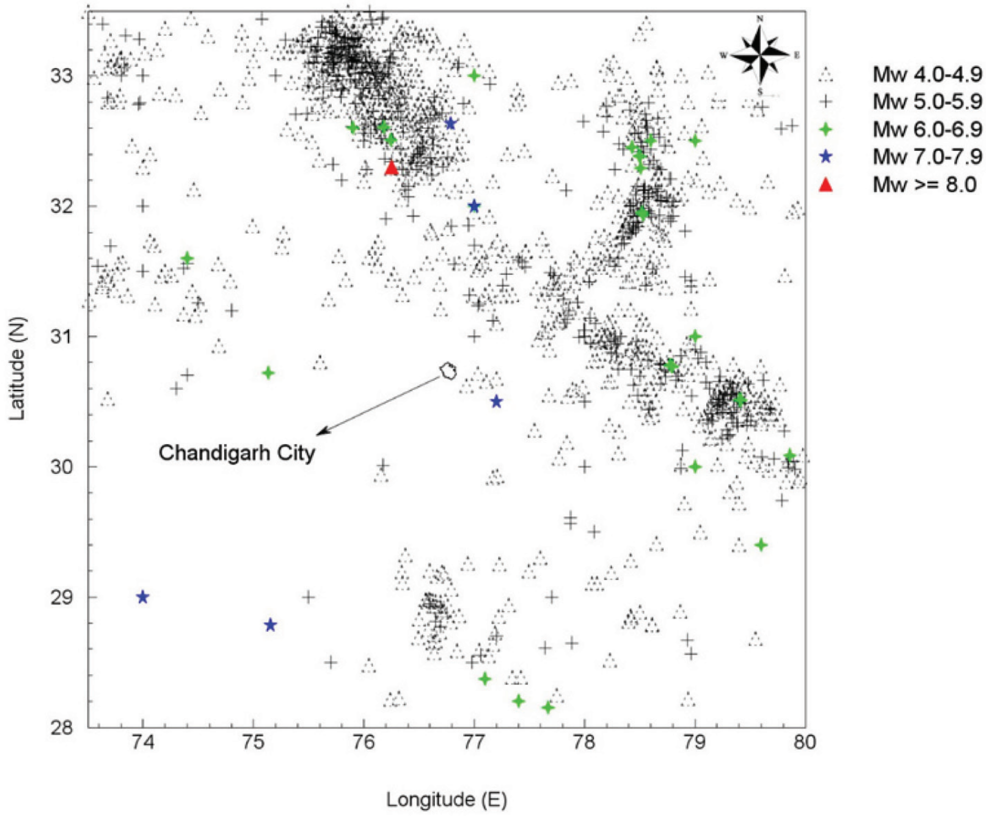

Figure 1. Epicenter map of the studied region situated around Chandigarh city.

Table 3. Completeness analysis of catalogue.

Magnitude Class (M_w)	CUVI method		Stepp method	
	Period	Interval (Years)	Period	Interval (Years)
4.0-4.9	1962-2015	53	1963-2015	52
5.0-5.9	1926-2015	89	1925-2015	90
6.0-6.9	1901-1975	74	1900-1970	70
7.0-7.9	1905-1999	94	1904-1999	95

3 respectively. The completeness periods as obtained by both the methods are quite comparable (Table 3). The catalogue is found to be complete for a sufficient period of time.

A tectonic map of the study area is prepared using Seismotectonic Atlas of India and its Environs (SEISAT) (Dasgupta et al., 2000) (Figure 4). SEISAT lists all the linear tectonic features which may or may not be active. Twenty tectonic features are identified which are likely to produce substantial ground motions. This has been done by overlaying epicenters of recorded events on the tectonic map.

Gutenberg-Richter seismicity parameters (a and b)

The seismicity parameters 'a' and 'b' are the key input parameters for PSHA. For simplicity, the study region has been divided into three sub-regions considering each sub-region as an area source of earthquakes. Considering the complete part of the catalogue for all the magnitude ranges, the seismicity parameters have been calculated for each area source through linear least squares regression method following an exponential distribution of magnitude as shown in Figures 5 to 7. The exponential distribution is given in equation (1) below:

$$\lambda_m = 10^{a-bM_w} = \exp(\alpha - \beta M_w) \qquad (1)$$

where λ_m = mean annual rate of exceedance, a = coefficient such that a^{th} power of 10 gives the mean yearly number of earthquakes of magnitude greater than or equal to zero, α = 2.303a, b = coefficient which describes the relative likelihood of large and small earthquakes and β = 2.303b. The reciprocal of the annual rate of exceedance (λ_m) for a particular magnitude is commonly referred to as the return period (T_R) of an earthquake exceeding that magnitude and is very important for earthquake resistant design. The

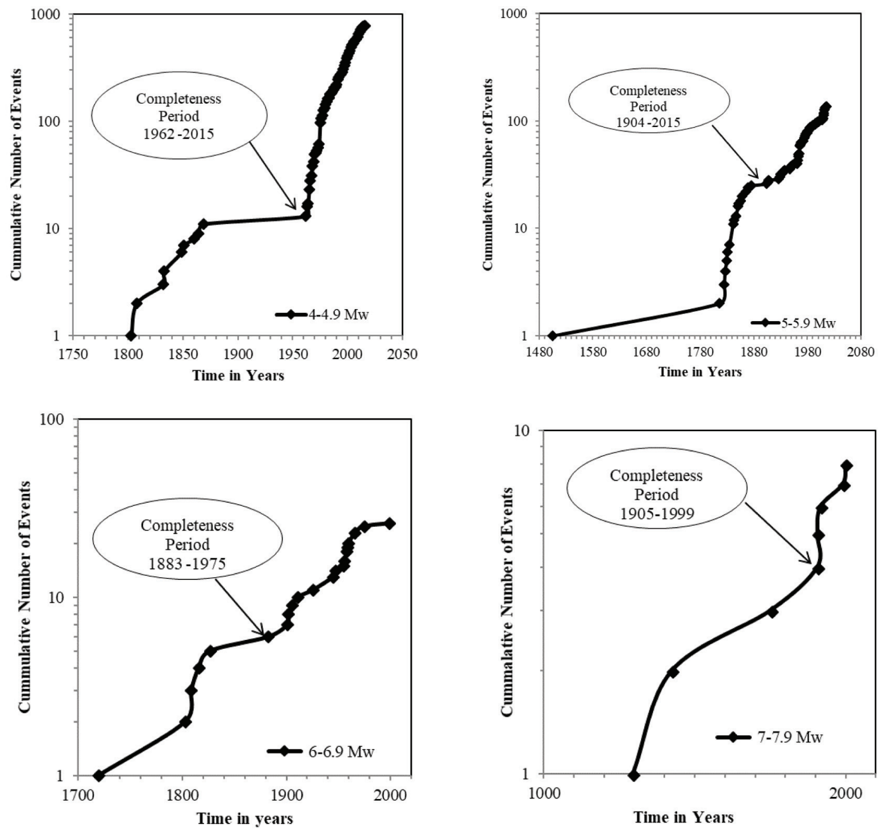

Figure 2. Completeness analysis using CUVI method.

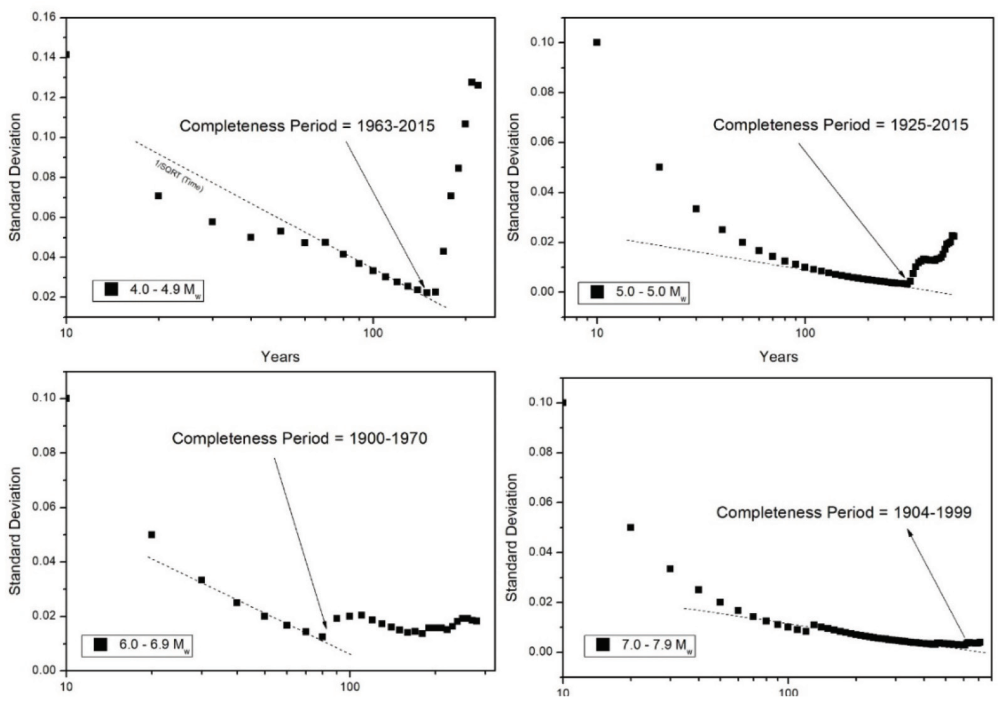

Figure 3. Completeness analysis using Stepp (1972) method.

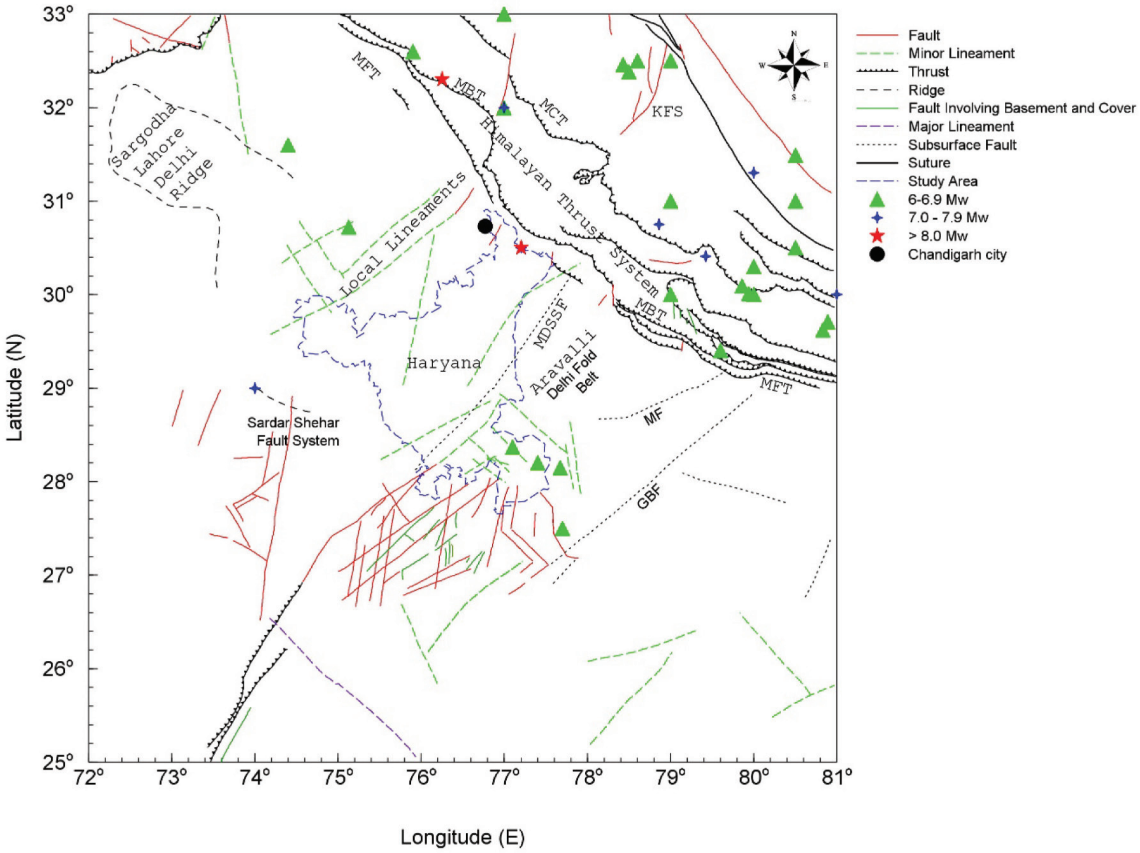

Figure 4. Tectonic map showing detailed tectonic features alongwith epicenter of significant earthquakes in the study region (after Dasgupta et al., 2000).

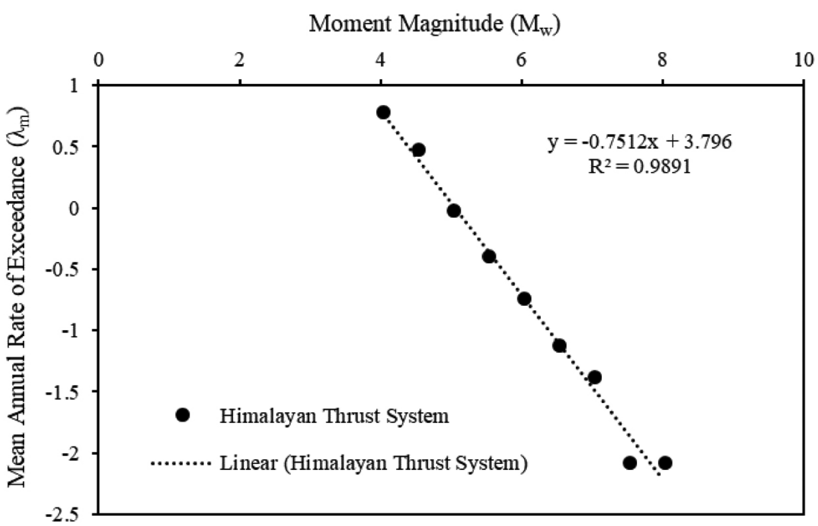

Figure 5. Seismicity parameters for Himalayan Thrust System.

seismicity parameters estimated along with the typical return periods for M_{obs} for all the area sources have been reported in Table 4. The value of return period calculated for different area sources demonstrates the capability of tectonic sources in Himalayan Thrust System to generate frequent large earthquakes.

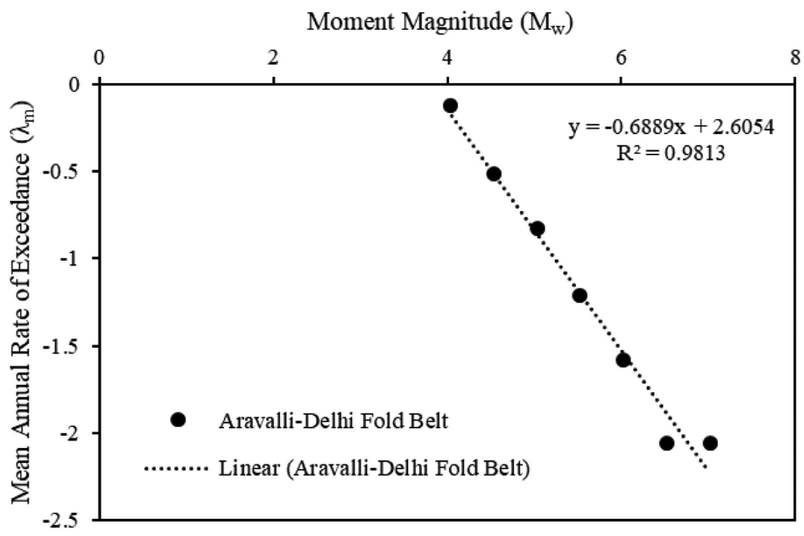

Figure 6. Seismicity parameters for Aravalli-Delhi Fold Belt.

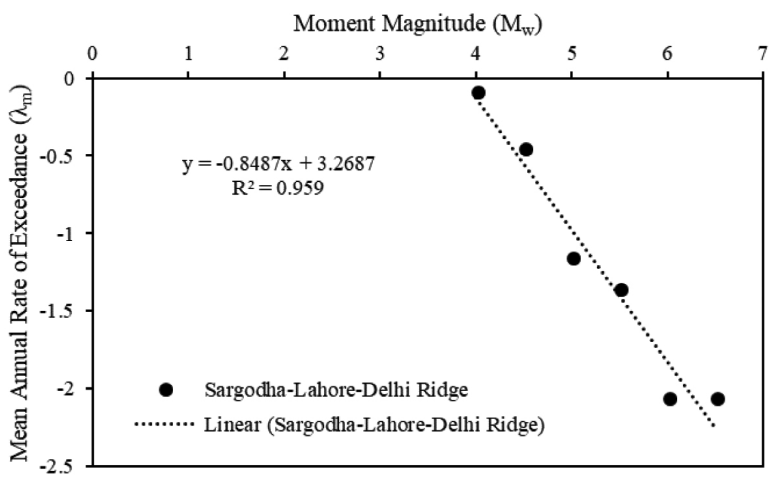

Figure 7. Seismicity parameters for Sargodha-Lahore-Delhi Ridge.

Table 4. Seismicity parameters for different area sources.

Area source	b	a	Range of magnitude (M_w) class	R^2	M_{obs}	Return Period (T_R) for M_{obs} (in years)
Himalayan Thrust System	0.75	3.8	4.0-8.0	0.989	8.0	159
Aravalli-Delhi Fold Belt	0.69	2.61	4.0-7.0	0.981	7.1	195
Sargodha-Lahore-Delhi Ridge	0.85	3.27	4.0-6.5	0.959	6.5	180

Estimation of maximum credible earthquake magnitude (M_{max})

Maximum credible earthquake magnitude (M_{max}) earthquakes for different seismogenic sources are estimated using appropriate empirical relations (Table 5). Total fault length (TFL) for various seismogenic sources are estimated. The sub-surface rupture length (RL) is considered as 1/3 of the TFL (Mark, 1977).

To estimate maximum credible earthquake magnitude (M_{max}), an increment of 0.5 is added to the maximum observed magnitude, wherever the available methods are not applicable (Gupta, 2002). Maximum observed magnitudes (M_{obs}) for various seismogenic sources are shown in Table 6. The maximum credible earthquake magnitudes (M_{max}) estimated for various seismogenic sources in the seismic study area are found to range from 5.1 to 8.5 (Table 7).

Table 5. Methods for estimating $M_{max.}$

Source	Empirical Relation	Magnitude Range	Total Fault Length (km)
Wells and Coppersmith (1994)	Mw=4.38+1.49 log(RL)	M_w 4.8 to 8.1	0 - 350
Bonilla et al., (1984)	Ms=6.04+0.708 log(RL)	M_s > 6.0	0 - 444
Vakov (1996)	Ms=4.422+1.448 log(RL)	M_w 4.5 to 8.5	0 - 470

Table 6. Earthquakes with maximum observed magnitude (M_{obs}) at the active seismogenic sources.

S.No.	Seismogenic Source	M_{obs}
1.	Main Boundary Thrust (MBT)	8.0
2.	Lineament System of Delhi Sargodha Ridge (LSDSR)	6.1
3.	Ropar Fault (RF)	5.0
4.	Fault Near Chandigarh (FNC)	4.6
5.	Jwala Mukhi Thrust (JMT)	5.5
6.	Main Frontal Thrust (MFT)	5.5
7.	Mahendragarh Dehradun Sub Surface Fault (MDSSF)	5.4
8.	Rohtak Dehradun Lineament (RDL)	5.0
9.	Main Central Thrust (MCT)	7.9
10.	Sardar Shahar Fault (SSF)	7.1
11.	Kaurik Fault (KF)	6.9
12.	Ramgarh Thrust (RT)	6.0
13.	Moradabad Fault (MF)	5.8
14.	Great Boundary Fault (GBF)	4.9
15.	North Almora Thrust (NAT)	5.7
16.	South Almora Thrust (SAT)	4.4
17.	Delhi Fold Belt (DFB)	6.7
18.	Aravalli Delhi Fold Belt (ADFB)	4.5
19.	Sundar Nagar Fault (SNF)	7.0
20.	Sargoda Lahore Delhi Ridge (SLDR)	6.5

Table 7. M_{max} for potential seismogenic sources.

Seismogenic Source	TFL (km)	RL (km)	**Bonilla et al. (1984)**	**Wells and Coppersmith (1994)**	**Vakov (1996)**	**Gupta (2002)**	M_{max}
MBT	825	275	-	-	-	8.5	8.5
LSDSR	97	32.33	-	-	-	6.6	6.6
RF	38	12.66	6.9	6.1	6.1	5.5	6.9
FNC	36	12	-	-	-	5.1	5.1
JMT	387	129	7.6	-	7.5	6.0	7.6
MFT	46	15.33	6.9	6.2	6.2	6.0	6.9
MDSSF	297	99	7.5	7.4	7.4	5.9	7.5
RDL	202	67.33	-	-	-	5.5	5.5
MCT	769	256.33	-	-	-	8.4	8.4
SSF	271	90.33	7.5	7.3	7.3	7.6	7.6
KF	120	40	7.2	6.8	6.8	7.4	7.4
RT	37	12.33	6.9	6.1	6.1	6.5	6.9
MF	162	54	7.3	7	7	6.3	7.3
GBF	316	105.33	7.5	7.4	7.4	5.4	7.4
NAT	280	93.33	7.5	7.4	7.3	6.2	7.5
SAT	130	43.33	7.3	-	6.9	4.9	7.3
ADFB	Area Source	-	-	-	-	7.2	7.2
SNF	101	33.67	7.2	6.7	6.7	7.5	7.5
SLDR	Area Source	-	-	-	-	7.0	7.0

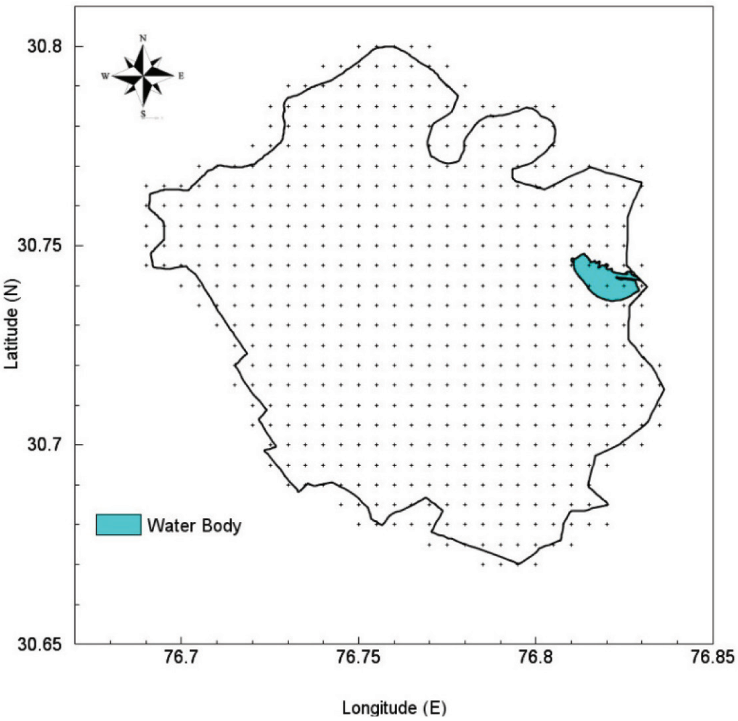

Figure 8. The map shows 549 grid points covering the entire area of Chandigarh city.

SEISMIC HAZARD ANALYSIS

A complete seismic hazard analysis involves various steps including preparation of comprehensive earthquake catalogue, identification of potential seismogenic sources, calculation of seismicity parameters a and b, estimation of M_{max} of the tectonic features, selection of suitable Ground Motion Prediction Equation (GMPE) and development of hazard map. Seismic hazard is estimated using probabilistic approach. The PSHA is considered to be more reliable as it provides a framework to accommodate uncertainties in size, location and rate of occurrence of earthquakes using total probability theorem. The detailed procedure for PSHA was first given by Cornell (1968) and explained in detail recently by Baker (2008).

The ground motion model is generally developed on the basis of strong motion characteristics of the region (plate boundary, subduction and intraplate) and accelerogram records at different epicentral distances for different magnitude of earthquakes. A regression analysis is then carried out based on different PGA values considering the distances and magnitudes to get the mean value of acceleration with minimum variance and subsequently, site coefficients are calculated for different periods. Due to scarcity of strong motion data, only a few region-specific attenuation relations are developed. Globally available GMPEs (Douglas, 2014) are reviewed to select equations suitable for the study region.

The following GMPE developed by Abrahamson and Silva (1997) for regions prone to shallow crustal earthquakes is adopted for the study area.

$$\ln Sa(g) = f_1(M, r_{rup}) + Ff_3(M) + HWf_4(M, r_{rup}) + Sf_5(\widehat{PGA}_{rock}) \quad (2)$$

where Sa(g) is spectral acceleration in g, M is moment magnitude, r_{rup} is closest distance to rupture plane in km, F is fault type (1 for reverse, 0.5 for reverse/oblique and 0 otherwise), HW is dummy variable for hanging wall sites (1 for sites over the hanging wall, 0 otherwise), and S is dummy variable for site class (0 for rock or shallow soil, 1 for deep soil).

for $M \le c_1$

$$f_1(M, r_{rup}) = a_1 + a_2(M - c_1) + a_{12}(8.5 - M)^n + [a_3 + a_{13}(M - c_1)] \ln R$$

for $M > c_1$ (3)

$$f_1(M, r_{rup}) = a_1 + a_4(M - c_1) + a_{12}(8.5 - M)^n + [a_3 + a_{13}(M - c_1)] \ln R$$

where $\sqrt{r_{rup}^2 + c_4^2}$, a_1-a_{13}, c_1, c_4, c_5, a_1-a_{13}, c_1, c_4, c_5 and n are site coefficients.

A grid of 0.005° × 0.005° (0.555 km × 0.555 km) is used for the entire area of the Chandigarh city (Figure 8). The PSHA is carried out considering three sub-regions, viz. Himalayan Thrust System, Sargodha-Lahore-Delhi Ridge and Aravalli-Delhi Fold Belt as area sources of earthquakes and based on the developed catalogue, average focal depths are taken as 15 km, 17 km and 10 km for the selected three sub-regions, respectively.

The hazard has been calculated for 1%, 2% and 10% probability of exceedance in a time frame of 50 years as per the recommendations of Eurocode 8 (2005). For ordinary

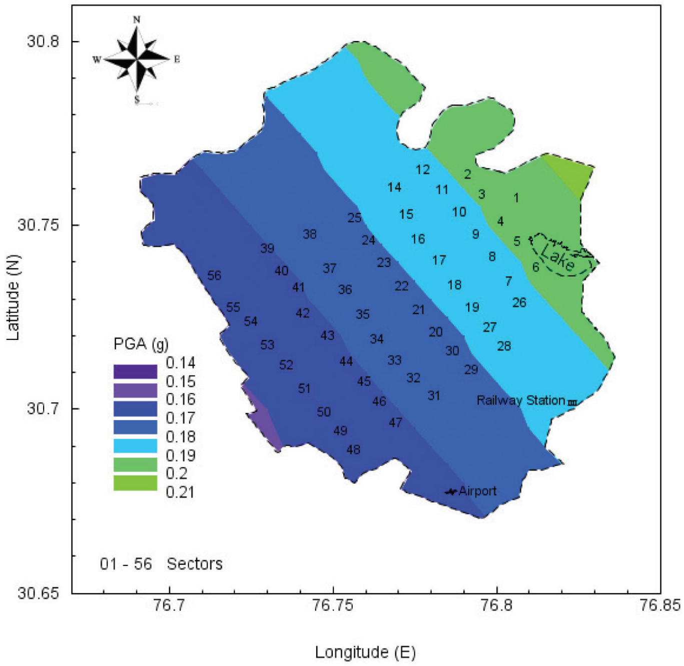

Figure 9. Seismic hazard map of Chandigarh city for 10% probability of exceedance in 50 years (return period of 475 years).

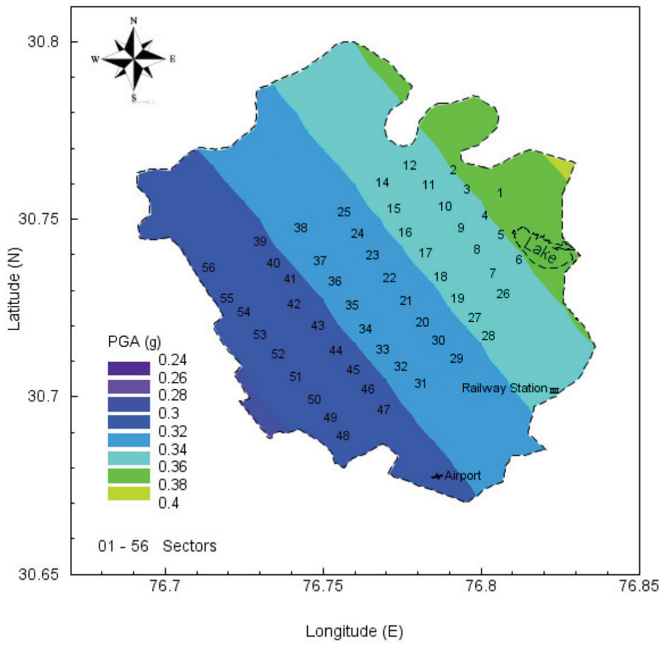

Figure 10. Seismic hazard map of Chandigarh city for 2% probability of exceedance in 50 years (return period of 2475 years).

structures, the seismic hazard map corresponding to 10% probability of exceedance in 50 years is recommended. However, for important structures like Nuclear Power Plants and other megastructures, the seismic hazard maps corresponding to 2% and 1% probability of exceedance in 50 years are recommended. The PSHA software R-CRISIS v. 18.2 (Ordaz and Salgado-Gálvez, 2017) is used for the purpose. R-CRISIS is a Windows based software with the capability of performing probabilistic seismic hazard analysis (PSHA), using a fully probabilistic approach allowing the calculation of results in terms of outputs with different characteristics (i.e., exceedance probability plots, set of stochastic events). In the computational scheme of the program, parameters such as a, b, M_{min}, M_{max}, λ_m and attenuation models are the input parameters, and PGA and PSA are the outputs.

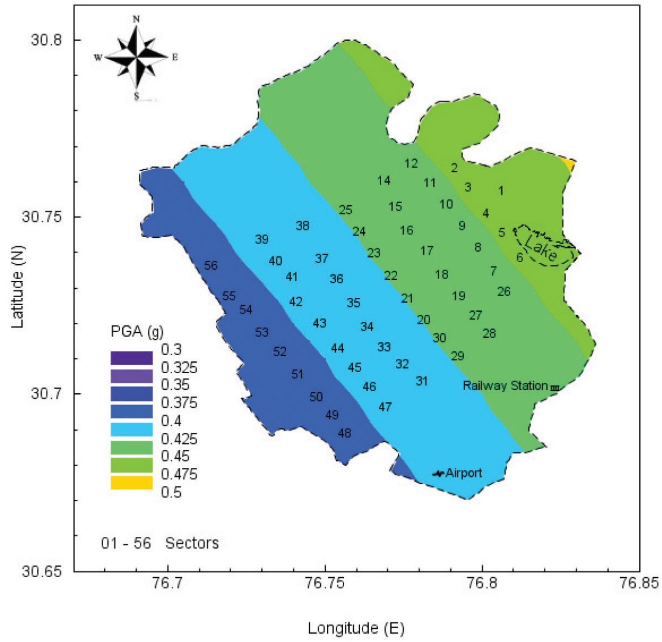

Figure 11. Seismic hazard map of Chandigarh city for 1% probability of exceedance in 50 years (return period of 4975 years).

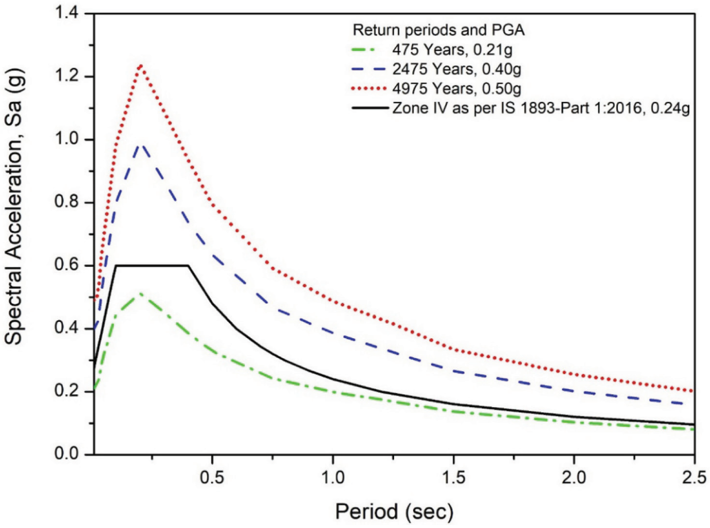

Figure 12. Response spectra for different return periods on rock outcrop corresponding to maximum PGA observed for Chandigarh.

The estimated PGA values range from 0.14g to 0.21g, 0.24g to 0.40g and 0.3g to 0.5g at 10%, 2% and 1% probability of exceedance respectively in 50 years. The hazard maps are prepared for 10%, 2% and 1% probability of exceedance at return periods of 475 years, 2475 years and 4975 years, respectively, in a time frame of 50 years (Figures 9 to 11). Response spectra is evaluated for various return periods corresponding to maximum observed PGA (Figure 12). It is observed that for a return period of 475 years, PSHA based hazard parameters are quite comparable with IS 1893 Part-1 (2016). For return periods of 2475 and 4975 years, PSHA based hazard parameters are much higher than the parameters specified in IS 1893 Part-1 (2016). For important structures, a site-specific approach is recommended due to possibility of amplification of ground motions for soil sites.

ONE-DIMENSIONAL NONLINEAR WAVE AMPLIFICATION

There are a number of analyses available to estimate the degree of wave amplification, e.g. linear, equivalent linear and non-linear analysis offering varying dimensionality (1-D, 2-D and 3-D) based on the problem. Over the years, nonlinear method is evolved to give a precise characterization of the nonlinear behaviour of soil (Stewart and Kwok, 2008). Generally, amplification of seismic waves is evaluated using one-dimensional model, which assumes that horizontal shear waves originating from the bedrock propagate in vertical direction through several layers of the soil profile. In line with various wave amplification studies carried out in India (e.g. Desai and Choudhury, 2015; Dammala et al., 2017), one dimensional nonlinear model is adopted to estimate wave amplification at soil sites of Chandigarh city using DEEPSOIL software (Hashash et al., 2016). This software is a one-dimensional site response analysis program that can perform: (a) 1-D nonlinear time domain analyses with and without pore water pressure generation, and (b) 1-D equivalent linear frequency domain analyses including convolution and deconvolution. The calculation of response is described below.

The nonlinear analysis of the wave propagation equation in soils allows the soil properties to change with the time with variation in strain. All the sites are assumed to have horizontal layers which extend infinitely. The soil profiles have been modelled as a series of lumped masses connected by springs and dashpots making a multiple degree freedom system. The nonlinear dynamic analysis of the soil column is performed by solving the incremental dynamic equation of motion as follows:

$$M\Delta\ddot{u} + C\Delta\dot{u} + K\Delta u = -M\Delta\ddot{u}_g \tag{4}$$

where the coefficients M, C and K represent mass, viscous damping and stiffness respectively and $\ddot{u}$, u, $\dot{u}$, $\ddot{u}_g$ represent acceleration, velocity, displacement and exciting acceleration at the base respectively.

The soil response is obtained from a constitutive model that describes the cyclic behaviour of soil. The most widely used softwares use variation of hyperbolic model to represent the backbone curve of the soil with the extended unload-reload Masing rules (Masing, 1926) to model hysteretic behaviour. The loading and unloading equations of modified Konder-Zelasko (MKZ) model (Matasovic, 1993), further modified by Hashash and Park (2001) used in DEEPSOIL software are as follows:

$$\tau = \frac{\gamma G_{max}}{1 + \beta\left(\frac{\gamma}{\gamma_r}\right)^S} \tag{5}$$

$$\tau = \frac{2G_{max}\left(\frac{\gamma - \gamma_{rev}}{2}\right)}{1 + \beta\left(\frac{\gamma - \gamma_{rev}}{2\gamma_r}\right)^S} + \tau_{rev} \tag{6}$$

where τ = shear strength, G_{max} = low strain shear modulus, γ = shear strain, reference shear strain, τ_{rev} = shear stress at reversal, γ_{rev} = shear strain at reversal, β, S = model fitting parameters.

The modification in MKZ model allows the effect of confining pressure on secant shear modulus of soil. In addition, there is no coupling between the confining pressure and shear stress. Coupling is introduced by making reference shear strain (γ_r) effective stress dependent using the following equation:

$$\gamma_r = a\left(\frac{\sigma'_v}{\sigma_{ref}}\right)^b \tag{7}$$

where a and b are curve fitting parameters, τ'_v = vertical effective stress, τ_{ref} = reference shear stress of 0.18 MPa.

However, the modified model is almost linear at low strains and hence provides zero hysteretic damping at lower strains. Low strain damping (ξ) is added separately to simulate actual soil behavior which exhibits damping even at very small strains and is defined as

$$\xi = \frac{c}{(\sigma'_v)^d} \tag{8}$$

where c and d are curve fitting parameters. The parameter 'd' can be set to zero in case a pressure independent small strain damping is desired.

It is observed that overestimation of damping at large strain can result when the hysteretic damping is calculated using unload-reload cycles as per Masing rules based on the modulus reduction curves. This overestimation can be avoided by multiplying ξ_{Masing} with a damping reduction factor $F(\gamma_m)$ as follows:

$$F(\gamma_m) = p_1 - p_2\left(1 - \frac{G_{\gamma_m}}{G_{max}}\right)^{p_3} \tag{9}$$

where $G\gamma_m$ = shear modulus at maximum strain and p_1, p_2, p_3 are fitting parameters. This factor provides the best fit for both modulus reduction and damping ratio curves.

The reduction factor modifies the reloading cycle and the expression is as follows:

$$\tau = F(\gamma_m)\left[\frac{2G_{max}\left(\frac{\gamma-\gamma_{rev}}{2}\right)}{1+\beta\left(\frac{\gamma-\gamma_{rev}}{2\gamma_r}\right)^S} - \frac{G_{max}\,(\gamma-\gamma_{rev})}{1+\beta\left(\frac{\gamma_m}{\gamma_r}\right)^S}\right] + \frac{G_{max}\,(\gamma-\gamma_{rev})}{1+\beta\left(\frac{\gamma_m}{\gamma_r}\right)^S} + \tau_{rev} \tag{10}$$

where γ_m = maximum shear strain. The Newmark β method is then used to solve the system of equations and to obtain response of the soil column.

Such analysis has been carried out for 8 sites in Chandigarh, which includes 4 sites with boreholes drilled up to refusal and others drilled down to depth of 20 m or greater (Figure 13).

Based on geotechnical data collected, sites are classified as class D sites by calculating average SPT N-value of the profile as per the recommendations of NEHRP (FEMA 368, 2000). The stiffness and damping of soil layer play fundamental role in estimating wave amplification parameters in seismic microzonation studies. The analysis requires characterization of the stiffness of an element of soil considering low strain shear modulus (G_{max}), variation of modulus ratio (G/G_{max}) with cyclic strain amplitude (γ) and other parameters. For this, several correlations between shear modulus (G) and SPT N-value for different soil types are considered. In the present study, the following equations developed by Ohba and Toriumi (1970) and Ohsaki and Iwasaki (1973) are used for clays and sands respectively, as per recommendations of Anbazhagan et al., (2012, 2015b, 2016):

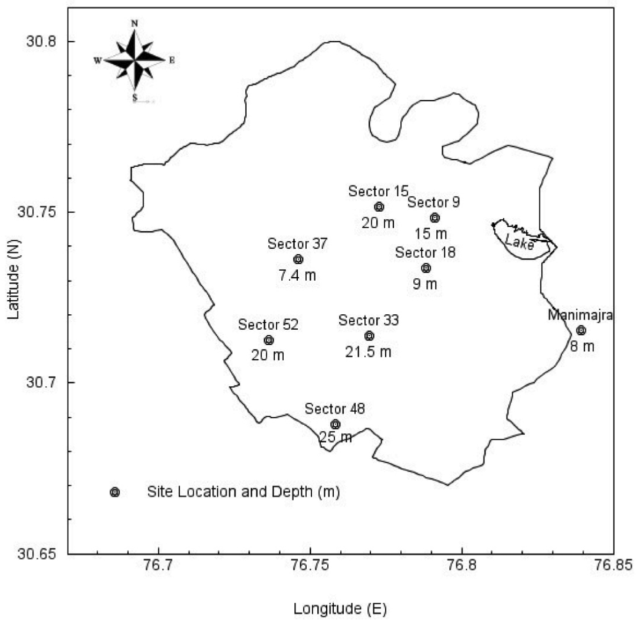

Figure 12. Response spectra for different return periods on rock outcrop corresponding to maximum PGA observed for Chandigarh.

Table 8. Input parameters for soil column at Sector 33.

Depth	IS Symbol	Plasticity Index	Bulk Density	SPT N Value	Angle of internal friction (φ)	Coefficient of earth pressure at rest (K_o)	G_{max} (MPa)
2.5	ML	2	15.47	8	28.63	0.52	43.43
3.5	ML-CL	7	17.43	7	28.31	0.53	39.98
5	ML	2	17.58	9	28.94	0.52	46.72
7	ML-CL	7	18.05	15	30.81	0.49	64.13
8	CL	9	18.68	23	33.31	0.45	83.59
9	CL	9	18.21	17	31.44	0.48	69.30
10	SM	NP	17.54	30	35.50	0.42	155.93
12.5	SM	NP	16.03	14	30.50	0.49	76.17
14	SM	NP	16.41	18	31.75	0.47	96.47
15	CL	9	18.99	27	34.56	0.43	92.33
15.8	CL	9	20.25	43	39.56	0.36	123.21
17	SM	NP	20.11	48	41.13	0.34	242.55
19	SM	NP	17.54	30	35.50	0.42	155.93
21.5	SM	NP	20.38	50	41.75	0.33	252.04

$$G_{max}=1220N^{0.62} \tag{11}$$

$$G_{max}=650N^{0.94} \tag{12}$$

where G_{max} = low strain shear modulus in t/m^2 and N = SPT-N value.

In the absence of site specific modulus reduction and damping ratio curves, standard curves proposed by Darendeli (2001) are used for sands, and curves proposed by Vucetic and Dobry (1991) are used for clays. Typical input parameters for the site in Sector 33 are given in Table 8.

The thickness of the layers is so adjusted that the maximum frequency that a layer can propagate is always above 25 Hz. Bedrock has been assumed at refusal, i.e. for N>50 for 15 cm penetration and N>100 for 30 cm penetration of SPT split-spoon sampler. Conventionally, the engineering bedrock is assumed to be the uppermost layer of the soil column having a shear wave velocity (V_s) ≥ 760 m/s in accordance with NEHRP provisions (Nath and Thingbaijam, 2011). In general, the shear wave velocity

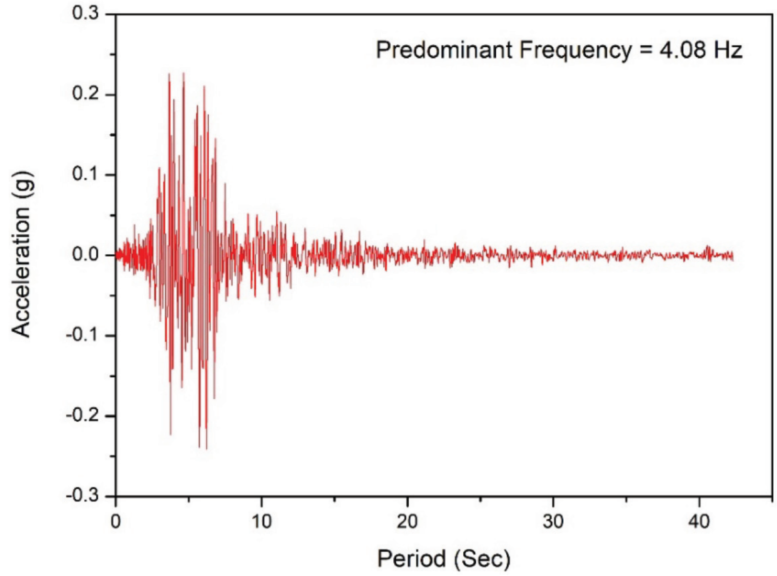

Figure 14. Input acceleration time history of the 1991 Uttarkashi earthquake 6.8 M_w (source: http://www.strongmotioncenter.org).

Table 9. Results of nonlinear wave amplification analysis.

Sites	PGA Rock (g)	Depth (m)	Site Class	Natural Frequency of Site (Hz)	Amplification Factor	PGA Soil (g)	Ground Displacement (m)	Maximum Strain	
								Value (%)	Depth (m)
Manimajra	0.191	9	D	7.04	1.583	0.302	0.010	0.46	5.5
Sector 09	0.188	15	D	3.42	1.186	0.223	0.020	1.12	5.5
Sector 15	0.183	20	D	2.16	1.165	0.213	0.030	1.75	16.5
Sector 18	0.183	9	D	5.82	1.736	0.318	0.011	0.35	4.5
Sector 33	0.173	21.5	D	2.49	0.963	0.167	0.025	0.54	11.5
Sector 37	0.172	7.4	D	6.81	1.963	0.338	0.012	0.64	2.5
Sector 48	0.164	25	D	2.06	0.748	0.123	0.036	1.52	19.5
Sector 52	0.165	20	D	2.54	0.777	0.128	0.031	0.63	13.5

of the bedrock is greater than that of the overlying soil profile. It should be noted that regardless of the value specified, the bedrock damping ratio has no effect in time domain analyses and only a negligible effect in frequency domain analyses (Hashash et al., 2016). For the present study, bedrock is modelled as an elastic half space with 2% damping, 2.5 gm/cm^3 density and 760 m/s shear wave velocity (V_s).

The final step in wave amplification analysis involves generating or getting an acceleration time history, which is compatible with the maximum dynamic loading expected at the site of interest. Suitable acceleration time histories can be selected based on PGA value, magnitude of controlling earthquake, source to site distance and site class. PGA values for rock sites obtained from PSHA are used for the selection of input motions at each site. Acceleration time history of the 1991 Uttarkashi earthquake M_w 6.8 (focal depth = 10 km) recorded at the Uttarkashi station with PGA = 0.242g is used for the analysis (Figure 14).

The results of the wave amplification analysis have been reported in Table 9. Due to limited borehole data (eight boreholes), interpretation cannot be made for the amplification trend across the city. However, on the basis of significant amplification observed at five sites, it can be concluded that the city may experience high ground accelerations. Moreover, high strains are observed for all the eight sites and there is a possibility of substantial settlements during an earthquake.

The amplification factors for the analysed sites range from 0.748 to 1.963 with an average value of 1.3. The maximum PGA of 0.338g and minimum PGA of 0.123g are observed for Sector 37 and Sector 48 sites, respectively. The seismic hazard map at return period of 475 years is updated using average observed amplification factor for PGA (Figure 15). The response spectrum corresponding to a return period of 475 year is modified using average observed amplification factors for Sa (Figure 16). It is observed that the response spectrum developed for soil sites

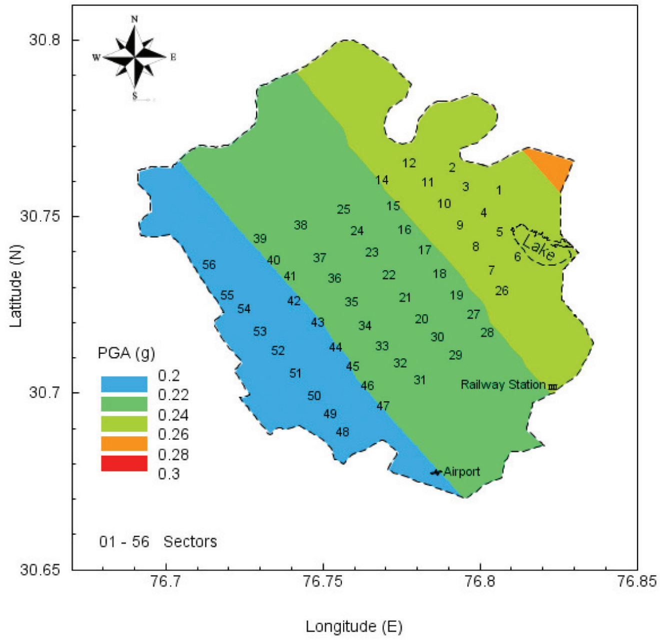

Figure 15. Seismic hazard map of Chandigarh city for 10% probability of exceedance in 50 years (return period of 475 years).

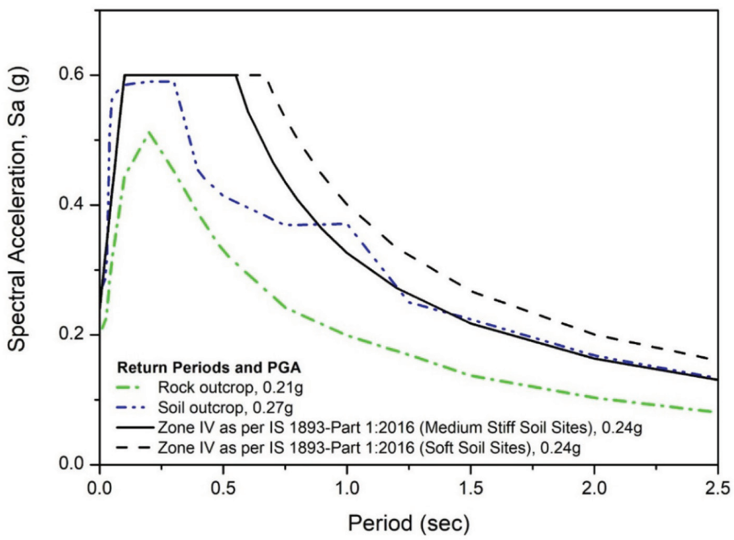

Figure 16. Comparison of response spectrum for rock and soil outcrop with soil response spectra specified in IS 1893 Part-1 (2016).

of Chandigarh is comparable with the spectrum specified in IS 1893 Part-1 (2016) for medium stiff soil sites. It is observed that the estimated seismic scenario for the Chandigarh city is worse than that proposed by the Indian Seismic Code (IS 1893 Part-1, 2016).

LIQUEFACTION HAZARD MAPPING

Liquefaction hazard assessment for Chandigarh city is carried out using semi-empirical procedure developed by Idriss and Boulanger (2006). The location of 41 boreholes are shown in Figure 17 and the profiles in Appendix A. For all the sites, water table has been assumed to be present at ground surface (NDMA, 2011; Vipin et al., 2013) and PGA and magnitude of earthquake (M_w) are taken as 0.28g and 8.228 respectively as per PSHA. Assessment of liquefaction susceptibility of soils requires calculation of cyclic stress ratio (CSR) which is the cyclic stress induced by an earthquake, and cyclic resistance ratio (CRR) which is the resistance offered by the soil against liquefaction.

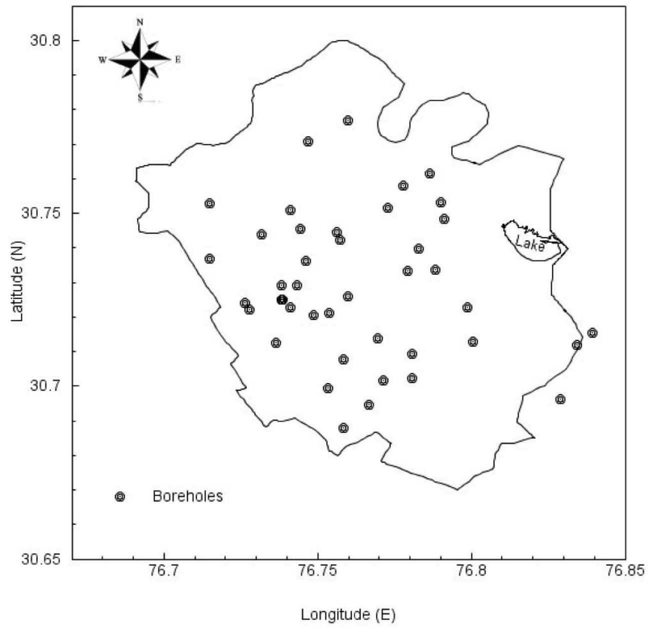

Figure 17. Map showing location of 41 boreholes.

Cyclic stress ratio (CSR)

It can be given by following equation:

$$(\mathrm{CSR})_{M=7.5,\sigma=1} = 0.65\left(\frac{\sigma_{vo}}{\sigma'_{vo}}\right)(a_{max})(r_d)\left(\frac{1}{MSF}\right)\left(\frac{1}{K_\sigma}\right) \quad (13)$$

where $(\mathrm{CSR})_{M=7.5,\ \sigma=1}$ is the adjusted value of CSR for equivalent uniform shear stress induced by earthquake ground motions having moment magnitude of 7.5 and equivalent overburden pressure of 1 atmosphere, σ_{vo}, = total overburden stress, σ'_{vo} = effective overburden stress, a_{max} = peak ground acceleration, r_d = stress reduction coefficient, MSF = magnitude scaling factor, K_σ = overburden correction factor, a_{max} = PGA corresponding to 475-year return period.

Stress reduction coefficient (r_d) accounts for the flexibility and dynamic response of the soil and represents the variation of shear stress amplitude with depth which can be given as:

$$r_d = \exp(\alpha + \beta M) \quad (14)$$

where,

$$\alpha = -1.012 - 1.126\sin\left(\frac{z}{11.73} + 5.133\right) \quad (15)$$

$$\beta = 0.106 + 0.118\sin\left(\frac{z}{11.28} + 5.142\right) \quad (16)$$

and z is depth and M is moment magnitude.
These equations are applicable for $z \le 34$m.
For $z > 34$m, the following expression is used:

$$r_d = 0.12\exp(0.22M) \quad (17)$$

Magnitude scaling factor (MSF) is used to adjust the CSR induced by an earthquake magnitude (M) to account for the duration effect of seismic ground motions, which is not reflected in PGA. The MSF is limited to a maximum value of 1.8 for small magnitude earthquakes of $M_w \le 5.4$ and is expressed as:

$$MSF = 6.9\exp\left(\frac{-M}{4}\right) - 0.058 \le 1.8 \quad (18)$$

Overburden correction factor is used to adjust CSR values to an equivalent overburden pressure of 1 atmosphere. Overburden correction factor (K_σ) is evaluated by the following expression:

$$K_\sigma = 1 - C_\sigma \ln(\sigma'_{vo}/P_a) \le 1.0 \quad (19)$$

$$C_\sigma = \frac{1}{18.9 - 2.55\sqrt{(N_1)_{60}}} \quad (20)$$

where P_a is the reference pressure.

Cyclic resistance ratio (CRR)

CRR can be represented by the following equation:

$$CRR = \left(CRR_{\sigma=1,\alpha=0}\right)K_\sigma K_\alpha \quad (21)$$

where K_σ = overburden correction factor and K_α = static shear stress correction factor.

The SPT N-values need to be normalized to an equivalent effective vertical overburden pressure σ'_{vo} of about 101 kPa to obtain blow count values that are more uniquely dependent on relative density (D_R), rather than on the overburden pressure coming from the above soil layers. The corrected blow count can be expressed as:

$$(N_1)_{60} = C_N(N)_{60} \quad (22)$$

$$C_N = \left(\frac{P_a}{\sigma'_{vo}}\right)^\alpha \le 1.7 \quad (23)$$

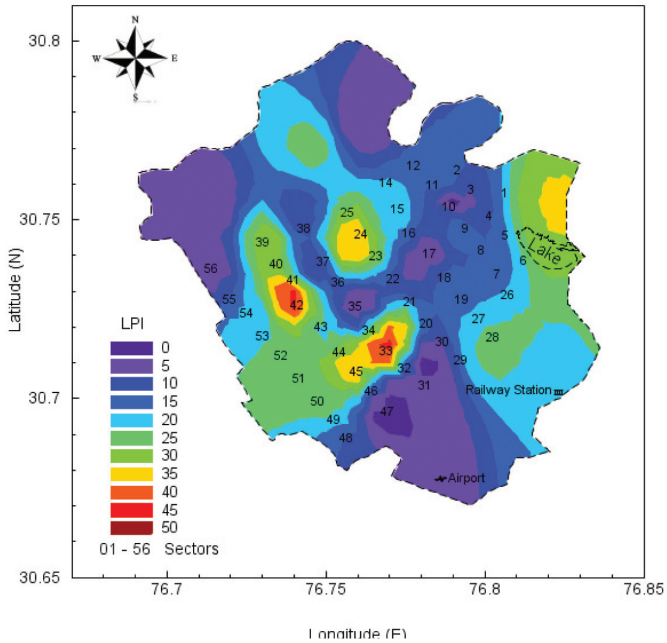

Figure 18. Liquefaction hazard map of Chandigarh city.

$$\alpha = 0.784 - 0.0768\sqrt{(N_1)_{60}} \tag{24}$$

Where $N_1 = C_N(N_m)$, N_m is the SPT value at field, C_N = overburden correction factor to normalize SPT value, N_{60} = SPT value after correction to an equivalent 60% hammer efficiency. The value of $(N_1)_{60}$ is limited to 46. The calculation of C_N is iterative as both C_N and $(N_1)_{60}$ depend on each other. The expression for N_{60} is as follows:

$$N_{60} = N_m C_R C_S C_B E_m / 0.60 \tag{25}$$

Where C_R = rod length correction, C_S = sampling method correction, C_B = borehole diameter correction and E_m = hammer efficiency. The value of correction factors for N_{60} is adopted from Youd et al., (2001).

Presence of fine content (FC) in the soil plays a role in liquefaction; higher the FC percentage in the sediment more resistive it would be towards liquefaction. Therefore, FC correction has to be applied to $(N_1)_{60}$ if FC > 5% to convert it into equivalent clean sand value. The description of correction factor is as follows:

$$(N_1)_{60CS} = (N_1)_{60} + \Delta(N_1)_{60} \tag{26}$$

where

$$\Delta(N_1)_{60} = \exp\left\{1.63 + \frac{9.7}{FC + 0.1} - \left(\frac{15.7}{FC + 0.1}\right)^2\right\} \tag{27}$$

for FC ≤ 35. These $(N_1)_{60cs}$ values are further used to compute CRR by using the following formulation:

$$CRR_{\sigma=1,\alpha=0} = \exp\left\{\frac{(N1)60cs}{14.1} + \left(\frac{(N1)60cs}{126}\right)^2 - \left(\frac{(N1)60cs}{23.6}\right)^3 + \left(\frac{(N1)60cs}{25.4}\right)^4 - 2.8\right\} \tag{28}$$

However, the layers with FC > 35% are considered non-liquefiable.

Factor of Safety and Liquefaction Potential Index (LPI)

The factor of safety (FOS) against liquefaction is determined as follows:

$$FOS = \frac{CRR}{CSR} \tag{29}$$

The FOS shows the potential of a given layer of soil against liquefaction. Generally, if the FOS value is less than 1, the site is considered to be liquefiable and if it is greater than 1, the site is considered to be non-liquefiable. However, soil that has a FOS slightly greater than 1.0 may still liquefy during an earthquake. For example, if a lower layer liquefies, then the upward flow of water could induce liquefaction of the layer that has a factor of safety slightly greater than 1.0.

On the other hand, liquefaction potential index (LPI) quantifies the severity of liquefaction at a given location for down to a depth of 20m (Iwasaki et al., 1978; Luna and Frost, 1998). It is computed by taking integration of one minus the factors of safety (FOS) against liquefaction for liquefiable layers along the entire depth of soil column below the ground surface at a specific location. The LPI value is considered zero for a layer with FOS ≥1. A weighting function has also been added to give more weight to the layers closer to the ground surface. The LPI is calculated using the following expression:

$$LPI = \sum_{i=1}^{n} w_i F_i H_i \tag{30}$$

Table 10. Liquefaction severity.

LPI	Severity of Liquefaction
LPI = 0	Little to None
0 < LPI < 5	Minor
5 < LPI < 15	Moderate
LPI > 15	Major

Table 11. Liquefaction potential index (LPI) for various sites in Chandigarh city.

Sites	Borehole Depth (m)	PGA Soil (g)	LPI	Severity
Village Sarangpur	9	0.242	5.00	Moderate
Village Mauli Jagram	6	0.241	20.16	Major
Village Manimajra	9	0.248	25.48	Major
Village Maloya	10	0.218	5.58	Moderate
Village Kaimbwala	9	0.235	35.45	Major
Sector 9	15	0.244	20.61	Major
Sector 10	12	0.246	0	None
Sector 11	9	0.247	18.78	Major
Sector 15	20	0.238	22.52	Major
Sector 17	12	0.238	4.52	Minor
Sector18	9	0.238	17.19	Major
Sector 24	9	0.230	39.94	Major
Sector 28	9	0.237	26.09	Major
Sector 31	15	0.225	6.26	Moderate
Sector 32	9	0.228	2.78	Minor
Sector 33	21.5	0.225	46.83	Major
Sector 35	13	0.225	5.33	Moderate
Sector 37	7.4	0.224	9.2	Moderate
Sector 38	16	0.226	10.5	Moderate
Sector 39	9	0.221	34.17	Major
Sector 42D	9	0.221	47.26	Major
Sector 43	9	0.222	23.64	Major
Sector 45	9	0.220	38.25	Major
Sector 46	9	0.222	4.02	Minor
Sector 47	9	0.218	3.92	Minor
Sector 48	25	0.213	14.45	Moderate
Sector 50B	9	0.216	27.15	Major
Sector 52	20	0.215	27.21	Major
Sector 54A	9	0.215	20.28	Major
Sector 56	13.4	0.215	7.7	Moderate
Village Dhanas	15	0.235	27.17	Major

and

$$F_i = 1 - FOS \tag{31}$$

where H_i is thickness of the discretized soil layer, n is number of layers; F_i is liquefaction severity for i^{th} layer; FOS_i is the factor of safety for i^{th} layer; w_i is the weighting factor = 10 - $0.5z_i$ and z_i is the depth of i^{th} layer (m). The level of liquefaction severity with respect to LPI (Luna and Frost, 1998) is given in Table 10.

The LPI values calculated for various boreholes across the city are shown in Table 11. Based on the results, a liquefaction hazard map is prepared for the city (Figure 18). The liquefaction hazard map shows that the villages Mauli Jagram, Manimajra, Kaimbwala, Dhanas, Sectors 9, 11, 15, 18, 24, 28, 33, 39, 42, 43, 45, 50B, 52 and 54A are highly prone to liquefaction during earthquakes if water table is assumed to be present at ground level. The village Sarangpur, Maloya, Sectors 31, 35, 37, 38, 48 and 56 have moderate susceptibility towards liquefaction. However, areas like Sector 10, 17, 32, 46 and 47 have none to low susceptibility towards liquefaction.

CONCLUSION

Chandigarh is one of the important cities in India and is famous for its infrastructure, industries and tourism. The city is always under the threat from earthquakes due to its proximity to Himalayan frontal fault. Possible seismic hazards in the city is evaluated by probabilistic seismic hazard analysis (PSHA), wave amplification analysis and liquefaction potential assessment. The results are presented in terms of seismic hazard maps for various return periods, response spectra, peak ground acceleration, amplification factors and liquefaction hazards. The results show that the city can experience strong ground motions due to earthquakes in Himalayan thrust system. The expected PGA with 10% probability of exceedance is 0.28g. The average wave amplification factor for the analysed sites has been observed as 1.3. It has been observed that many areas in the city are prone to earthquake induced liquefaction. The results of the study can be useful for upcoming design and construction works in the city.

ACKNOWLEDGEMENT

Authors would like to acknowledge DST, India for providing financial assistance to carry out the study under INSPIRE Fellowship Scheme (Candidate Code IF130892). Authors would also acknowledge the help provided by UT Secretariat Chandigarh and Geotech Engineering Services (Mohali) by sharing geotechnical data for the study. Authors thank the anonymous reviewers for their valuable comments towards improving the quality of the manuscript.

Compliance with Ethical Standards

The authors declare that they have no conflict of interest and adhere to copyright norms.

REFERENCES

Abrahamson, N.A. and Silva, W.J., 1997. Empirical response spectral attenuation relations for shallow crustal earthquakes. Seism. Res. Lett., 68(1), 94-127.

Anbazhagan, P., Aditya, P. and Rashmi, H.N., 2012. Review of correlations between SPT N and shear modulus: a new correlation applicable to any region. Soil Dyn. Earthq. Eng., 36, 52-69.

Anbazhagan, P., Bajaj, K. and Patel, S., 2015a. Seismic hazard maps and spectrum for Patna considering region-specific seismotectonic parameters. Natural Hazards, 78, 1163-1195.

Anbazhagan, P., Manohar, D.R., Moustafa, S.S.R. and Nassir, S.A., 2015b. Effect of shear modulus correlation on site response study. Disaster Adv., 8(2), 16-30.

Anbazhagan, P., Manohar, D.R., Moustafa, S.S.R. and Nassir, S.A., 2016. Selection of shear modulus correlation for SPT N values based on site response analysis. J. Eng Res., 4(3), 18-42.

Baker, J.W., 2008. An Introduction to Probabilistic Seismic Hazard Analysis (PSHA), White Paper, Version 1.3, Stanford University, California.

https://scits.stanford.edu/sites/default/files/baker_2013_intro_psha_v2.pdf

Bonilla, M.G., Mark, R.K. and Lienkaemper, J.J., 1984. Statistical relations among earthquake magnitude, surface rupture length, and surface fault displacement. Bull. Seism. Soc. Am., 74(6), 2379-2411.

Boominathan, A., Dodagoudar, G.R., Suganthi, A. and Maheswari, U.R., 2008. Seismic hazard assessment of Chennai city considering local site effects. J. Earth System Sci., 117(2), 853-863.

Cetin, K.O., Seed, R.B., Kiureghian, A.D., Tokimatsu, K., Harder Jr., L.F., Kayen, R.E. and Moss, R.E.S., 2004. Standard penetration test-based probabilistic and deterministic assessment of seismic soil liquefaction potential. J. Geotech. Geoenviron. Eng., 130(12), 1314-1340.

Chopra, S., Kumar, D., Rastogi, B.K., Choudhury, P. and Yadav R.B.S., 2012. Deterministic seismic scenario for Gujrat region, India. Natural Hazards, 60, 517-540.

Cornell, C.A., 1968. Engineering seismic risk analysis. Bull. Seism. Soc. Am., 58, 1583-1606.

Dammala, P.K., Krishna, A.M., Bhattacharya, S., Nikitas, G. and Rouholamin, M., 2017. Dynamic soil properties for seismic ground response studies in Northeastern India. Soil Dyn. Earthq. Eng. 100, 357-370.

Darendeli, M.B., 2001. Development of a new family of normalized modulus reduction and material damping curves. Ph.D diss., University of Texas.

Dasgupta, S., Pande, P., Ganguly, D., Iqbal, Z., Sanyal, K., Venkatraman, N.V., Dasgupta, S., Sural, B., Harendranath, L., Mazumdar, K., Sanyal, S., Roy, A., Das, L.K., Misra, P.S. and Gupta, H., 2000. Seismotectonic atlas of India and its environment. Geol. Surv. India, Calcutta.

Desai, S.S. and Choudhury, D., 2015. Non-linear site-specific seismic ground response analysis for port sites in Mumbai, India. Japanese Geotech. Soc. Spl. Publ., 2(19), 733-736.

Douglas, J., 2014. Ground motion prediction equations 1964-2014. White paper, University of Strathclyde, Glasgow, United Kingdom. http://www.gmpe.org.uk/gmpereport2014.pdf

Eurocode 8: BS-EN 1998-1, 2005. Design of structures for earthquake resistance – part 1: General rules, seismic actions and rules for buildings. European committee for standardization, Brussels.

FEMA 368, 2000. National earthquake hazard reduction program (NEHRP) recommended provisions for seismic regulations for new buildings and other structures, part 1: Provisions. USA: Building Seismic Safety Council (BSSC).

Gardner, J.K. and Knopoff L., 1974. Is the sequence of earthquakes in Southern California with aftershocks removed, poissonian?. Bull. Seism. Soc. Am., 64(5), 1363–1367.

Gupta, I.D., 2002. The state of the art in seismic hazard analysis, ISET J. Earthq. Techn., 39(4), 311–346.

Hashash, Y.M.A. and Park, D., 2001. Non-linear one-dimensional seismic ground motion propagation in the Mississippi embayment. Eng. Geol., 62(1-3), 185-206.

Hashash, Y.M.A., Park, D., Tsai, C.C., Philips, C. and Groholski, D.R., 2016. DEEPSOIL - 1-D Wave Propagation Analysis Program, Version 6.1, Tutorial and User Manual. University of Illinois at Urbana-Campaign.

Idriss, I.M. and Boulanger, R.W., 2006. Semi-empirical Procedures for Evaluating Liquefaction Potential during Earthquakes. Soil Dyn. Earthq. Eng., 26, 115- 130.

Iwasaki, T., Tatsuoka, F., Tokida, K. and Yasuda, S., 1978. A practical method for assessing soil liquefaction potential based on case studies at various site in Japan. 5th Japan Earthquake Engineering Symposium, 2, 641-648.

IS 1893. Part-1, 2016. Criteria for Earthquake Resistant Design of Structures. Bureau of Indian Standard (BIS), New Delhi, India.

Kataria, N.P., Shrikhande, M. and Das, J.D., 2013. Deterministic seismic hazard analysis of Andaman and Nicobar Islands. J. Earthq. Tsunami., 7(4), 1-19.

Khattri K.N., Rogers A.M., Perkins D.M. and Algermissen S.T., 1984. A seismic hazard map of India and adjacent areas. Tectonophysics, 108, 93–134.

Kolathayar, S., Sitharam, T.G. and Vipin, K.S., 2012a. Deterministic seismic hazard macrozonation of India. J. Earth System Sci., 121(5), 1351-1364.

Kolathayar, S., Sitharam, T.G. and Vipin, K.S., 2012b. Spatial variation of seismicity parameters across India and adjoining areas. Natural Hazards, 60, 1365-1379.

Kramer, S.L., 2013. Geotechnical Earthquake Engineering. Pearson Publications.

Luna, R. and Frost, J.D., 1998. Spatial liquefaction analysis system J. Comput. Civil Eng., 12(1), 48-56.

Mark, R.K., 1977. Application of linear statistical model of earthquake magnitude versus fault length in estimating maximum expectable earthquake. Geology, 5, 464-466.

Malik, J.N., Nakata, T., Philip, G., Suresh, N. and Virdi, N.S., 2008. Active fault and paleoseismic investigation: evidence of a historic earthquake along Chandigarh Fault in the Frontal Himalayan zone, NW India. Himalayan Geology, 29(2), 109-117.

Malik, J.N., Shah, A.A., Sahoo, A.K., Puhan, Banerjee. C., Shinde D.P., Juyal N., Singhvi A.K. and Rath S.K., 2010. Active fault, fault growth and segment linkage along the Janauri anticline (frontal foreland fold), NW Himalaya, India. Tectonophysics, 483, 327–343.

Masing, G., 1926. Eigenspannungeu und verfertigung beim Messing. Proceedings of the 2nd Int. Cong. on Appl. Mech., Zurich, 332-335. (in German)

Matasovic, N., 1993. Seismic response of composite horizontally-layered soil deposits, Ph.D diss., University of California.

Molnar, P. and Pandey, M.R., 1989. Rupture zones of great earthquakes in the Himalayan region. Proc. Indian Acad. Sci. – Earth Planet. Sci., 98(1), 61-70.

Naik, N. and Choudhury, D., 2015. Deterministic seismic hazard analysis considering different seismicity levels for the state of Goa, India. Natural Hazards, 75, 557-580.

Nath, S.K. and Thingbaijam, K.K.S., 2011. Assessment of seismic site conditions: a case study from Guwahati city, northeast India. Pure Appl Geophys., 168, 1645-1668.

Nath S.K., Sengupta, P. and Kayal, J.R., 2002. Determination of S-Wave Site Response in the Garhwal Himalaya from the Aftershock Sequence of the 1999 Chamoli Earthquake. Bull. Seism. Soc. Am., 92(3), 1072-1081.

National Disaster Management Authority (NDMA), 2011. Geotechnical/geophysical investigations for seismic microzonation studies of urban centres in India. Technical report. Government of India.

Ohba, S. and Toriumi, I., 1970. Research on vibration characteristics of soil deposits in Osaka, Part 2, On velocities of wave propagation and predominant periods of soil deposits. Abstract, Technical meeting of Architectural Institute of Japan.

Ohsaki, Y. and Iwasaki, R., 1973. Dynamic shear moduli and Poisson's ratio of soil deposits. Soils and Foundations, 13(4), 61-73.

Ordaz M. and Salgado-Gálvez, M.A., 2017. R-CRISIS Validation and Verification Document. Technical Report, Mexico city, Mexico.

Peltzer, G. and Saucier, F., 1996. Present day kinematics of Asia derived from geological fault rates. J. Geophys. Res., 101, 27943 - 27956.

Puri, N. and Jain, A., 2014. Preliminary investigation for screening of liquefiable areas in the state of Haryana, India, ISET J. Earthq. Tech., 51(1-4), 19-34.

Potter, S.H., Becker, J.S., Johnston, D.M. and Rossiter, K.P., 2015. An overview of the impacts of the 2010-2011 Canterbury earthquakes, Int. J. Disaster Risk Reduction, 14, 6-14.

Puri, N. and Jain, A., 2016. Deterministic Seismic Hazard Analysis for the State of Haryana, India. Indian Geotech. J., 46(2), 164-174.

Rajendran, C.P. and Rajendran, K., 2005. The status of central seismic gap: a perspective based on the spatial and temporal aspects of the large Himalayan earthquakes. Tectonophysics, 395(1-2), 19-39.

Ranjan, R., 2005. Seismic Response Analysis of Dehradun city, India. MS Thesis, International Institute for Geo-information Science and Earth Observation, Netherlands.

Scordilis, E.M., 2006. Empirical global relations converting Ms and mb to moment magnitude, J. Seismology, 10, 225-236.

Sharma, M.L., Wason, H.R., and Dimri, R., 2003. Seismic zonation of Delhi region for bedrock ground motion. Pure. Appl. Geophys., 160, 2381-2398.

Shiuly, A., and Narayan, J.P., 2012. Deterministic seismic microzonation of Kolkata city, Natural Hazards, 60, 223-240.

Shukla, J. and Choudhury, D., 2012. Estimation of seismic ground motions using deterministic approach for major cities of Gujarat, Natural Hazards. Earth System Sci., 12, 2019-2037.

Sitharam, T.G. and Sil, A., 2014. Comprehensive seismic hazard assessment of Tripura and Mizoram states. J. Earth System Sci., 123(4), 837-857.

Stewart, J.P. and Kwok, A.O.L., 2008. Nonlinear seismic ground response analysis: code usage protocols and verification against vertical array data, Proceedings of Geotechnical Earthquake Engineering and Soil Dynamics IV Congress, Sacramento, California.

Stepp, J.C., 1972. Analysis of the completeness of the earthquake sample in the Puget Sound area and its effects on statistical estimates of earthquakes hazard, Proc. Int. Conf. on Microzonation for Safer Construction Research and Application, Seattle, Washington.

Thaker, T.P., Rathod, G.W., Rao, K.S. and Gupta, K.K., 2012. Use of seismotectonic information for the seismic hazard analysis for Surat city, Gujrat, India: Deterministic and probabilistic approach. Pure. Appl. Geophys., 169, 37-54.

Tinti, S. and Mulargia, F., 1985. Completeness analysis of a seismic catalog. Annales Geophysicae, 3(3), 407-414.

Tokimatsu, K., and Uchida, A., 1990. Correlation between liquefaction resistance and shear wave velocity, Soils and Foundations, 30(2), 33-42.

Vakov, A.V., 1996. Relationships between earthquake magnitude, source geometry and slip mechanism. Tectonophysics, 261(1), 97-113.

Vipin, K.S., Sitharam, T.G. and Kolathayar, S., 2013. Assessment of seismic hazard and liquefaction potential of Gujarat based on probabilistic approaches, Natural Hazards 65, 1179–1195.

Vucetic, M. and Dobry, R., 1991. Effect of Soil Plasticity on Cyclic Response, J. Geotech. Eng. Div., 111(1), 89-107.

Wells, D.L. and Coppersmith, K.J., 1994. New empirical relationships among magnitude, rupture length, rupture area, and surface displacement, Bull. Seism. Soc. Am., 84(4), 974-1002.

Yenier, E., Erdoğan, Ö. and Akkar, S., 2008. Empirical relationships for magnitude and source-to-site distance conversions using recently compiled Turkish strong-ground motion database, Proceedings of 14th World Conf. on Earthquake Engineering, Beijing, China.

Youd, T.L., Idriss, I.M., Andrus, R.D., Arango, I., Castro, G., Christian, J.T. and Dobry, R. et al., 2001. Liquefaction resistance of soils: summary report from the 1996 NCEER and 1998 NCEER/NSF workshops on evaluation of liquefaction resistance of soils, J. Geotech. Geoenviron. Eng., 127(10), 817–33.

Received on: 17.4.18; Revised on: 19.6.18; Accepted on: 15.7.18

Appendix-A: Borehole logs showing depth (m) and IS Classification of soil at various locations in Chandigarh city